

LOCKHEED MISSILES & SPACE COMPANY, INC.
HUNTSVILLE RESEARCH & ENGINEERING CENTER
HUNTSVILLE RESEARCH PARK
4800 BRADFORD DRIVE, HUNTSVILLE, ALABAMA

SUBSTRUCTURING
TECHNIQUES

Contract NAS8-30520

CR-121051

October 1971

by

W. D. Whetstone

and

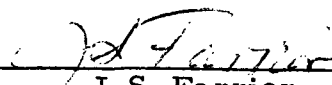
C. E. Jones

Prepared for National Aeronautics and Space Administration
Marshall Space Flight Center, Alabama 35812

APPROVED:



Donald McDonald, Manager
Structures & Mechanics Dept.



J. S. Farrior
Resident Director

SUMMARY

This report presents results of example problems solved using the Substructure Function Generator Program and the Substructure Synthesis Program, which are described in "Advanced Substructuring Techniques - Final Report," LMSC-HREC D225003.

To illustrate the advantages of "uniform acceleration modes" as substructure displacement functions, vibrational characteristics of a branched-beam model of a space shuttle launch vehicle were computed using several combinations of types of functions. The results were compared with essentially exact solutions computed by the dynamic analysis version of SNAP/V70F.

Also presented are results of a transient response analysis of the beam model, to illustrate the function of Substructure Synthesis Program's response routines.

CONTENTS

Section		Page
	SUMMARY	ii
1	INTRODUCTION	1
2	SUBSTRUCTURE DISPLACEMENT FUNCTIONS	3
3	TRANSIENT RESPONSE	18
4	REFERENCES	22

Section 1 INTRODUCTION

Reference 1 describes in detail the computer programs developed under Contract NAS8-30520.

The Substructure Function Generator Program is an adaptation of the Lockheed-Huntsville Structural Network Analysis Program, SNAP. Input to this program consists of a definition of a finite element model of a substructure, and specification of the type and number of displacement functions to be generated. Primary output is a substructure data file (tape, drum, etc.) containing the substructure mass and stiffness matrices expressing kinetic and potential energies as quadratic forms in coefficients of the displacement functions, etc.

The Substructure Synthesis program forms complete system mass, stiffness, and damping matrices, computes system modes and frequencies, and executes transient response calculations. Input to this program consists of the array of substructure data files generated by the Function Generator program for individual substructures, and data cards defining the position and interconnection of the substructures, damping data, forcing function details, function control parameters, etc., as described in detail in Ref. 1. The analyst also controls the particular sets of substructure displacement functions actually used by the Substructure Synthesis program in each analysis (i.e., not all of the functions stored in the substructure data files need be used in a given analysis).

The following types of substructure displacement functions are generated by the Function Generator Program:

1. Rigid body modes
2. Static functions associated with juncture node motion (called "restraint modes" in Refs. 2 and 3)
3. Undamped free vibrational modes
4. Arbitrary functions corresponding to any static loading specified by the analyst
5. Uniform acceleration modes.

The first four types of functions are widely used in various substructure/modal synthesis programs; however, the uniform acceleration modes (Whetstone, Ref. 4) apparently are not widely used at this time. The basis of these functions is reviewed in Section 2, and numerical results are given.

Section 2

SUBSTRUCTURE DISPLACEMENT FUNCTIONS

One of the objectives of the substructure/modal synthesis approach is to obtain relatively low-order system mass and stiffness matrices which represent with reasonable accuracy the low-frequency dynamics of large, complicated structures. If properly implemented, the procedure yields very accurate results; for example, Refs. 5 and 6 report calculations of Saturn IB and Saturn V launch vehicle lateral modes which closely agree with experimental data over a wide range of frequencies. Central problems arising in application of the procedure are (1) choice of the number, form, and composition of substructures, and (2) choice of substructure displacement functions. These choices are, of course, closely interrelated. If many small substructures are employed, fewer (and simpler) displacement functions may be used for each substructure than if only a few large substructures are used.

For a given system mode, the motion of any component substructure may be considered to be composed of rigid body motion plus deformation; that is, the motion of a point in the substructure may be written as $U \sin \omega t$, where

$$U = D + X R + \delta , \quad (1)$$

and

$$U = \begin{bmatrix} U_1 \\ U_2 \\ U_3 \end{bmatrix} , \quad D = \begin{bmatrix} D_1 \\ D_2 \\ D_3 \end{bmatrix} , \quad X = \begin{bmatrix} 0 & X_3 & -X_2 \\ -X_3 & 0 & X_1 \\ X_2 & -X_1 & 0 \end{bmatrix} , \quad R = \begin{bmatrix} R_1 \\ R_2 \\ R_3 \end{bmatrix} , \quad \text{and} \quad \delta = \begin{bmatrix} \delta_1 \\ \delta_2 \\ \delta_3 \end{bmatrix} . \quad (2)$$

In the above equations, U_i is the total direction i displacement of the point, the D_i 's and R_i 's are direction i rigid body displacement and rotation components, respectively, the X_i 's are position coordinates (right-hand, rectangular) of the point relative to the rotation center, and the δ_i 's represent deformation.

The dynamic forces acting on the substructure are (1) edge forces exerted by other substructures on the juncture nodes, and (2) distributed inertia forces. Where m is mass density, the inertia force distribution is proportional to $m \ddot{U}$. Accurate solutions will be obtained if, in addition to rigid body modes, we use as substructure displacement functions "static modes" corresponding to sets of static loadings which can closely approximate the actual dynamic forces. Static modes produced by unit motions of the juncture nodes (the previously-mentioned "restraint modes") are essential for this purpose. However, the customarily-used "fixed-constraint normal modes" generally do not provide a very good means of representing the effects of distributed inertia forces. A class of functions well-suited for this purpose may be identified through examination of the nature of the distributed inertia forces. If the substructures are sufficiently small, the third term (deformation) in Eq. (1) is small compared with the first two (rigid body motion). Accordingly, it is advantageous to include in each set of substructure displacement functions a set of functions representative of inertia force distributions associated with arbitrary rigid body motion. In general three-dimensional applications, six of these functions, which will be called "uniform acceleration modes" should be used. They are static modes produced by the following loading conditions:

- distributed forces equivalent to the inertia forces associated with constant linear acceleration of the substructure as a rigid body (i.e., dead weight loadings) in each of three non-parallel directions, and
- distributed forces equivalent to the inertia forces associated with constant angular acceleration of the substructure as a rigid body about each of three non-parallel axes.

All complete sets of rigid body modes, static modes associated with juncture node motion, and uniform acceleration modes are equivalent, regardless of the boundary conditions used in computing the uniform acceleration modes. That is, if a general three dimensional substructure contains n juncture nodes, a complete basis for constructing all such functions is provided by any set of displacement functions composed of (1) six independent rigid body modes, (2) $6(n-1)$ independent static modes associated with juncture node motion, and (3) six independent uniform acceleration modes (regardless of the restraint conditions imposed at the juncture nodes for purposes of computing the uniform acceleration modes).

Uniform acceleration modes are inexpensively calculated. Each one requires much less computer execution cost than a typical normal mode.

A convenient and meaningful measure of the accuracy of a system mode, as computed by the substructure technique (or any Rayleigh-Ritz method) is afforded by a comparison of the inertia force distribution as computed from equations of motion with the external force distribution computed from basic force-deflection (elasticity) relations. If the distributions so computed are equal, the solution is exact; if not, the difference is a measure of the constraint error associated with the particular set of displacement functions used. In this connection, it will be convenient to regard all substructure displacement functions as static modes (including vibrational modes, such as "fixed-constraint normal modes," which may be regarded as static modes produced by static loadings proportional to mass density times the function itself). The external (inertia) force distribution within each substructure, as computed from basic elastic relations, is a linear combination of the static force functions used to compute the substructure displacement functions. Accordingly, if only a small number of "fixed constraint normal modes" are used as substructure deformation functions, it is evident that the comparison of inertia forces with external forces computed from elastic relations generally cannot be very good, since the static loadings corresponding to such modes are identically zero at the juncture nodes. Use of a large number of such

normal modes will, of course, improve the quality of the inertia force approximation; however, this opposes the objective minimizing the number of degrees of freedom.

To indicate the effectiveness of uniform acceleration modes, the example shown on Fig. 1 was analyzed using four separate sets of substructure generalized functions, as summarized on Table 1. The results, which were compared with essentially exact solutions computed by the dynamic analysis version of SNAP, are summarized on Table 2. Only symmetric modes were computed.

All four cases included complete sets of six rigid body motions and six "restraint modes" (static functions corresponding to unit boundary motion components). Additional functions used in each case are summarized in the last four columns of Table 1, using the designations indicated below.

Uniform acceleration modes:

UX = Linear acceleration, direction X
 UY = Linear acceleration, direction Y
 UZ = Linear acceleration, direction Z
 \overline{UX} = Angular acceleration about axis X
 \overline{UY} = Angular acceleration about axis Y
 \overline{UZ} = Angular acceleration about axis Z

Fixed constraint normal modes:

NX1 First normal mode, bending in direction X
 NX2 Second normal mode, bending in direction X
 :
 :
 etc.

Each substructure contained three beam elements, as indicated in Table 1. In the model used in the SNAP/Dynamics analysis, structural joints were located at the ends of each of the beam elements.

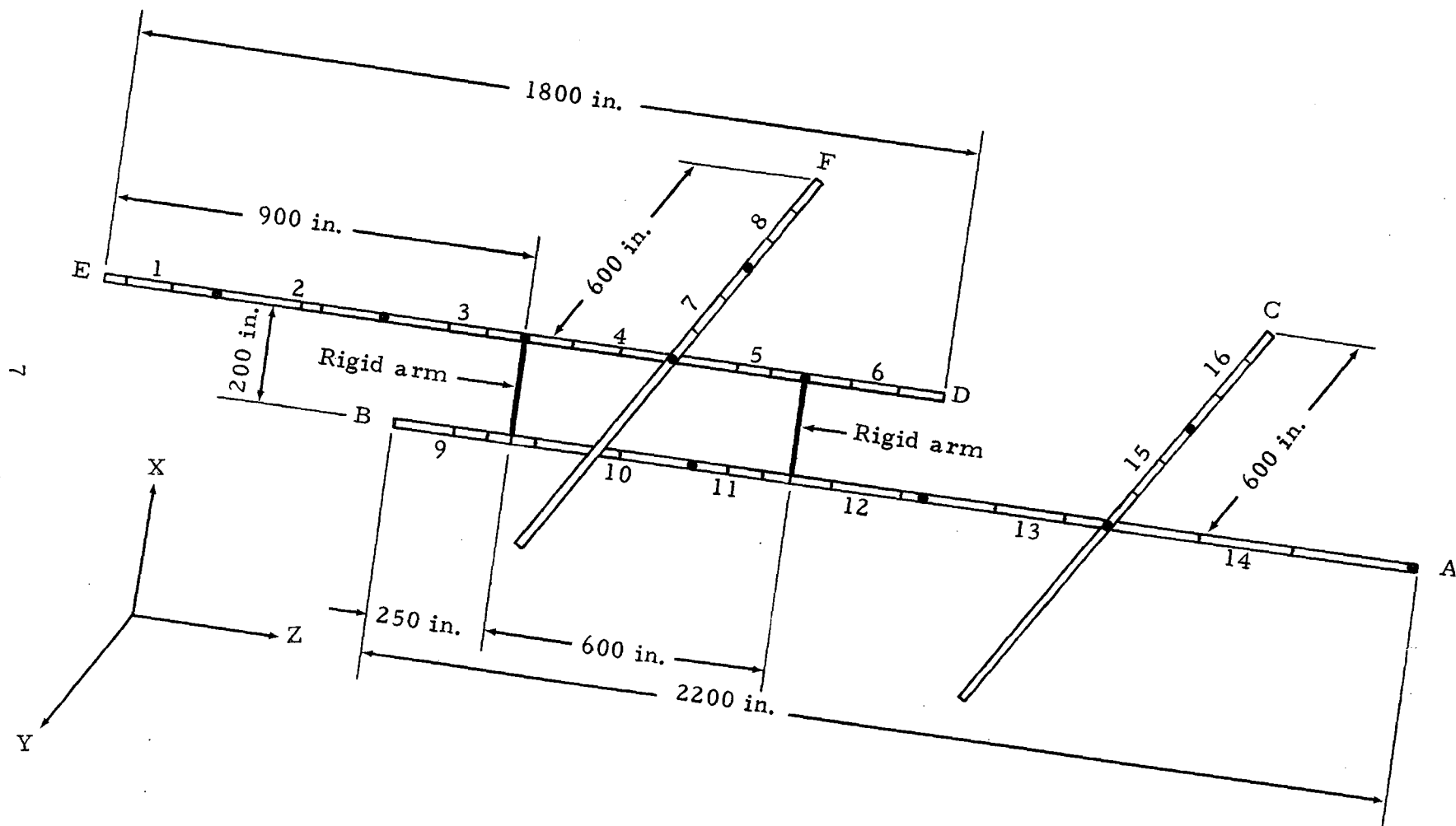


Fig. 1 - Beam Model of Space Shuttle Vehicle

Table 1
SUBSTRUCTURE CHARACTERISTICS

Substructure	Element	Length (in.)	Weight (lbs/in.)	Area (in. ²)	*Moment of Inertia (in. ⁴)	Generalized Function Sets			
						Case A	Case B	Case C	Case D
1	1	50	35	7.5	$.5 \times 10^5$	UX	NX1	UX	NX1
	2	100	35	20.5	$.15 \times 10^6$	<u>UZ</u>	NX2	<u>UZ</u>	NX2
	3	100	35	20.5	$.15 \times 10^6$	<u>UY</u>	UZ	<u>UY</u>	UZ
2	1	180	35	50.0	$.34 \times 10^6$	UX	NX1	<u>UX</u>	NX1
	2	40	35	70.0	$.46 \times 10^6$	<u>UZ</u>	NX2	<u>UY</u>	NX2
	3	130	920	70.0	$.46 \times 10^6$	<u>UY</u>	UZ		
3	1	140	948	70.0	$.46 \times 10^6$	UX	NX1	<u>UX</u>	NX1
	2	80	119	70.0	$.46 \times 10^6$	<u>UZ</u>	NX2	<u>UY</u>	NX2
	3	80	119	70.0	$.46 \times 10^6$	<u>UY</u>	UZ		
4	1	100	119	70.0	$.46 \times 10^6$	<u>UX</u>	NX1	<u>UX</u>	NX1
	2	100	119	70.0	$.46 \times 10^6$	<u>UY</u>	NX2	<u>UY</u>	NX2
	3	100	119	70.0	$.46 \times 10^6$				
5	1	140	119	53.0	$.46 \times 10^6$	UX	NX1	<u>UX</u>	NX1
	2	80	91	53.0	$.46 \times 10^6$	<u>UZ</u>	NX2	<u>UY</u>	NX2
	3	80	91	53.0	$.46 \times 10^6$	<u>UY</u>	UZ		
6	1	100	91	53.0	$.46 \times 10^6$	UX	NX1	UX	NX1
	2	100	35	53.0	$.46 \times 10^6$	<u>UZ</u>	NX2	<u>UZ</u>	NX2
	3	100	35	53.0	$.46 \times 10^6$	<u>UY</u>	UZ	<u>UY</u>	UZ
7	1	100	14	42.0	$.42 \times 10^4$	UX	NX1	UX	NX1
	2	100	12	36.0	$.35 \times 10^4$	<u>UZ</u>	NX2	<u>UZ</u>	NX2
	3	100	10	31.0	$.28 \times 10^4$	<u>UZ</u>	UZ	<u>UZ</u>	UZ
8	1	100	10	31.0	$.28 \times 10^4$	UX	NX1	UX	NX1
	2	100	8	26.0	$.21 \times 10^4$	UY	NX2	UY	NX2
	3	100	6	21.0	$.14 \times 10^4$	<u>UZ</u>	UY	<u>UZ</u>	UX2
						<u>UZ</u>	UZ	<u>UZ</u>	UZ

*Moments of inertia for substructures 7 and 8 are given about global axis Z. The moments of inertia about global axis X for these substructures were ten times those appearing in the table.

Table 1 (Continued)

Substructure	Element	Length (in.)	Weight (lbs/in.)	Area (in. ²)	*Moments of Inertia (in. ⁴)	Generalized Function Sets			
						Case A	Case B	Case C	Case D
9	1	130	59	27.0	$.56 \times 10^6$	UX	NX1	UX	NX1
	2	70	59	90.0	$.18 \times 10^7$	UZ	NX2	UZ	NX2
	3	50	59	90.0	$.18 \times 10^7$	UY	UZ	UY	UZ
10	1	50	59	125.0	$.18 \times 10^7$	UX	NX1	UX	NX1
	2	180	2659	125.0	$.25 \times 10^7$	UZ	NX2	UY	NX2
	3	170	2659	125.0	$.25 \times 10^7$	UY	UZ		
11	1	75	2659	125.0	$.25 \times 10^7$	UX	NX1	UX	NX1
	2	75	2659	125.0	$.25 \times 10^7$	UZ	NX2	UY	NX2
	3	50	224	138.0	$.28 \times 10^7$	UY	UZ		
12	1	100	224	138.0	$.28 \times 10^7$	UX	NX1	UX	NX1
	2	150	224	138.0	$.28 \times 10^7$	UY	NX2	UY	NX2
	3	50	224	138.0	$.28 \times 10^7$				
13	1	150	224	138.0	$.28 \times 10^7$	UX	NX1	UX	NX1
	2	150	224	138.0	$.28 \times 10^7$	UY	NX2	UY	NX2
	3	100	224	151.0	$.30 \times 10^7$				
14	1	200	224	151.0	$.30 \times 10^7$	UX	NX1	UX	NX1
	2	200	224	151.0	$.30 \times 10^7$	UZ	NX2	UY	NX2
	3	250	59	151.0	$.30 \times 10^7$	UY	UZ		
15	1	100	64	120.0	20×10^4	UX	NX1	UX	NX1
	2	100	54	105.0	6×10^4	UZ	NX2	UZ	NX2
	3	100	44	90.0	5×10^4	UZ	UZ	UZ	UZ
16	1	100	44	90.0	5×10^4	UX	NX1	UX	NX1
	2	100	34	75.0	1.4×10^4	UY	NX2	UY	NX2
	3	100	24	66.0	$.66 \times 10^4$	UZ	UY	UZ	UY
						UZ	UZ	UZ	UZ

*Moments of inertia for substructures 15 and 16 are given about global axis Z. The moments of inertia about global axis X for these structures were ten times those appearing in the table.

Table 2
COMPARISON OF SOLUTIONS

Mode	Solutions Computed by SNAP/Dynamics	Frequencies (Hz) Computed by Substructure Synthesis Program			
		Case A	Case B	Case C	Case D
4	2.16	2.16	2.16	2.16	2.16
5	2.69	2.69	2.69	2.69	2.69
6	5.40	5.40	5.40	5.40	5.40
7	5.63	5.63	5.63	5.63	5.63
8	6.82	6.82	6.82	6.82	6.82
9	7.75	7.75	7.75	7.83	7.83
10	9.21	9.21	9.21	9.47	9.47
11	11.16	11.16	11.16	11.17	11.17
12	11.29	11.29	11.29	11.33	11.33
13	14.79	14.79	14.79	14.83	14.83
14	16.01	16.04	16.04	17.21	17.21
15	17.69	17.72	17.72	18.89	18.89

Case A (lateral and longitudinal uniform acceleration modes) and Case B (lateral normal modes, longitudinal uniform acceleration modes) gave results practically identical to the almost exact solutions produced by SNAP/Dynamics. Longitudinal uniform acceleration modes were not included for interior substructures having uniform properties (i.e., substructures 4, 7, 12, 13, 15).

The results of Cases A and B are typical of similar comparisons involving other types of finite element nets. Normal modes are generally much more expensive to compute than uniform acceleration modes, but usually give equal (or less accurate) results, unless the structure is modeled by only a few large substructures.

Case C is the same as Case A, except that the longitudinal uniform acceleration modes are omitted entirely. Case D is similarly related to Case B. The effects of excluding all longitudinal uniform acceleration modes are most pronounced in modes 10, 14, and 15.

Plots of the mode shapes are shown on Figs. 2 through 13.

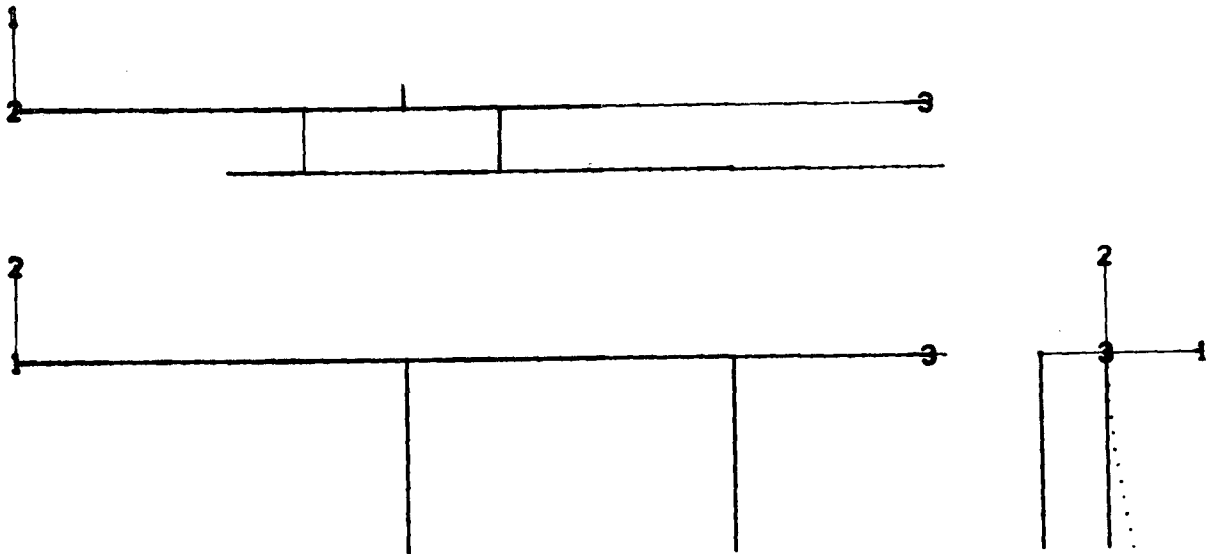


Fig. 2 - Mode 4, Frequency = 2.16 Hz

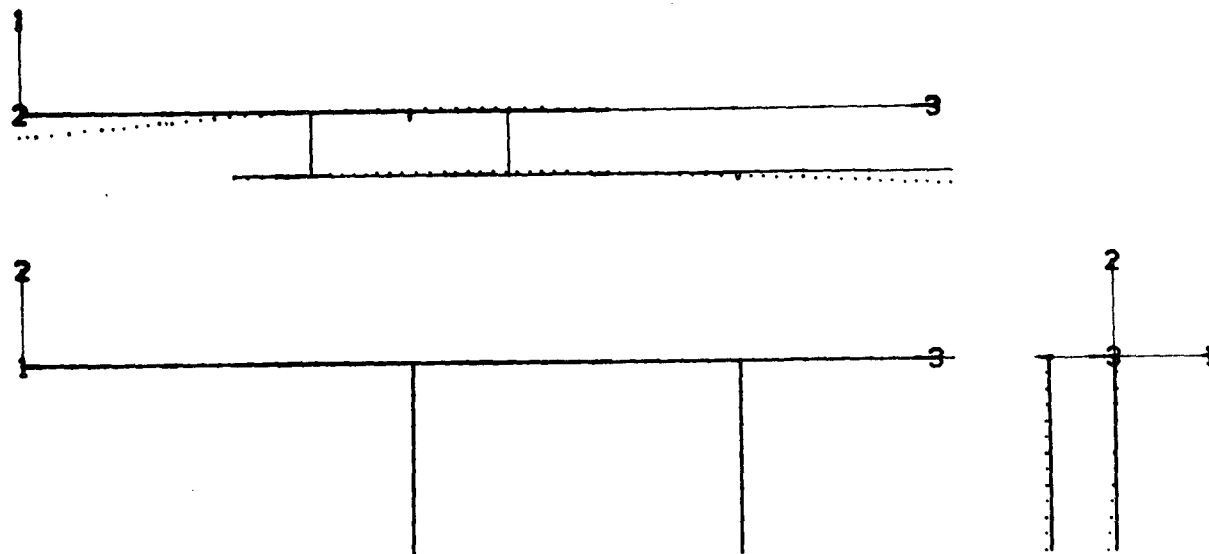


Fig. 3 - Mode 5, Frequency = 2.69 Hz

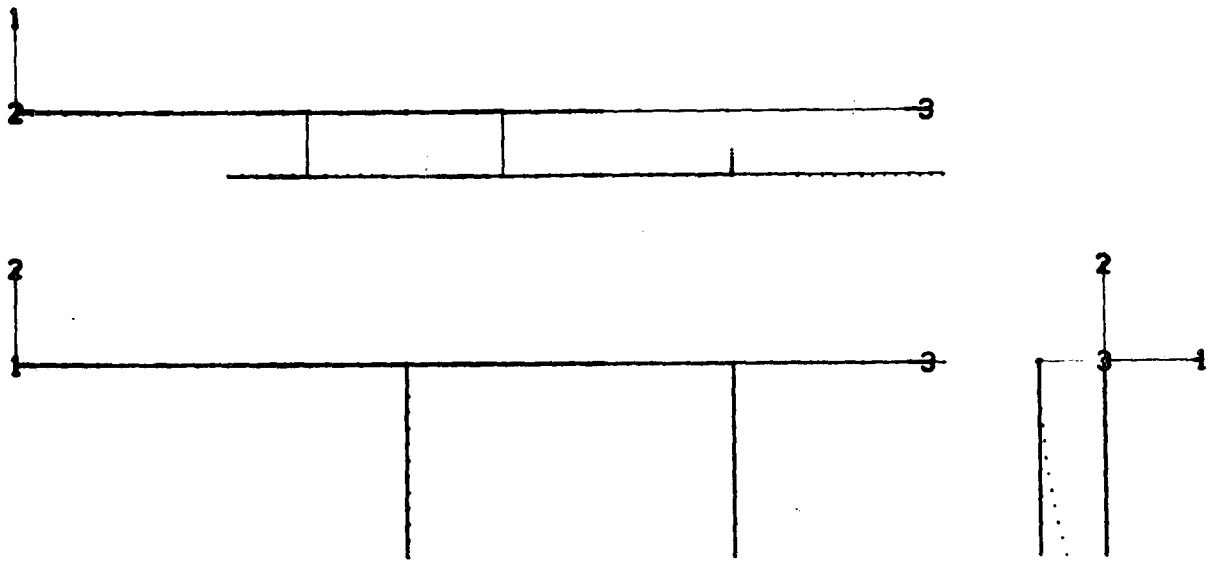


Fig. 4 - Mode 6, Frequency = 5.40 Hz

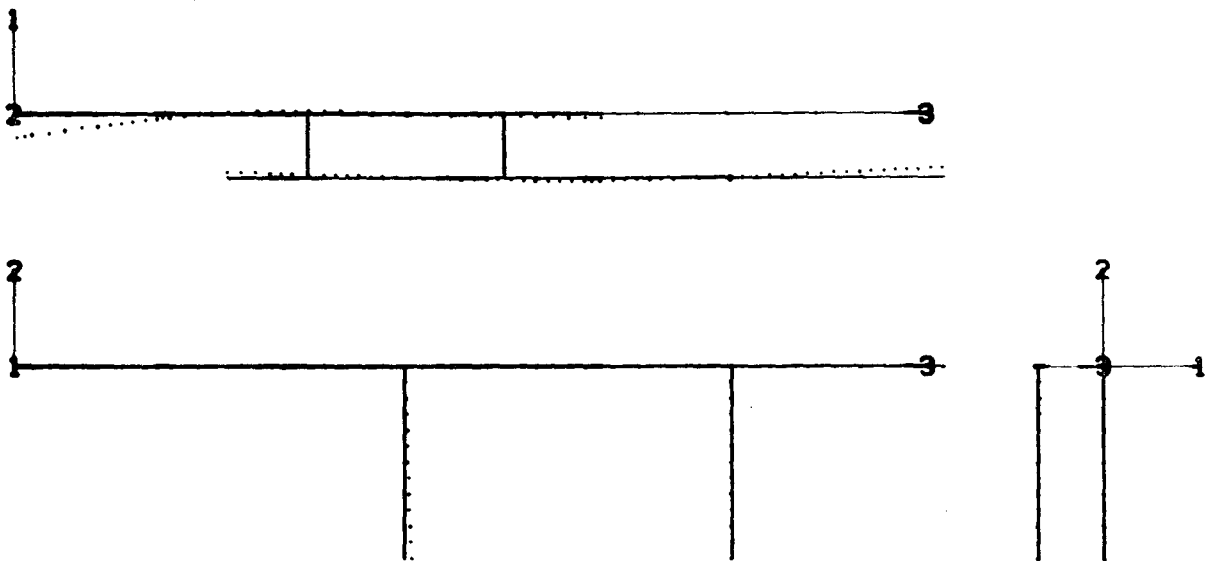


Fig. 5 - Mode 7, Frequency = 5.63 Hz

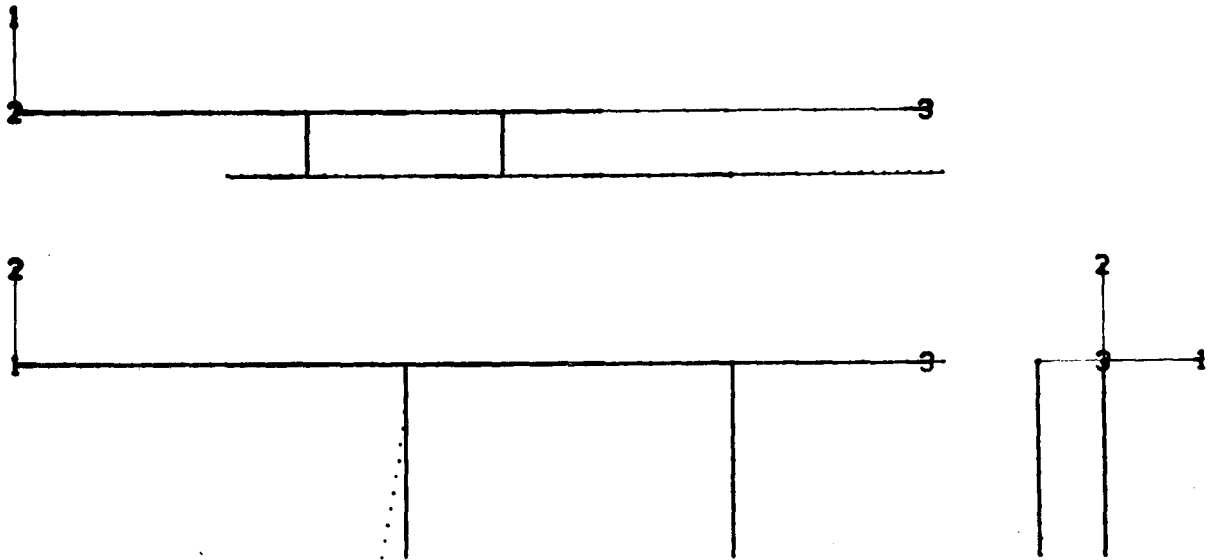


Fig. 6 - Mode 8, Frequency = 6.82 Hz

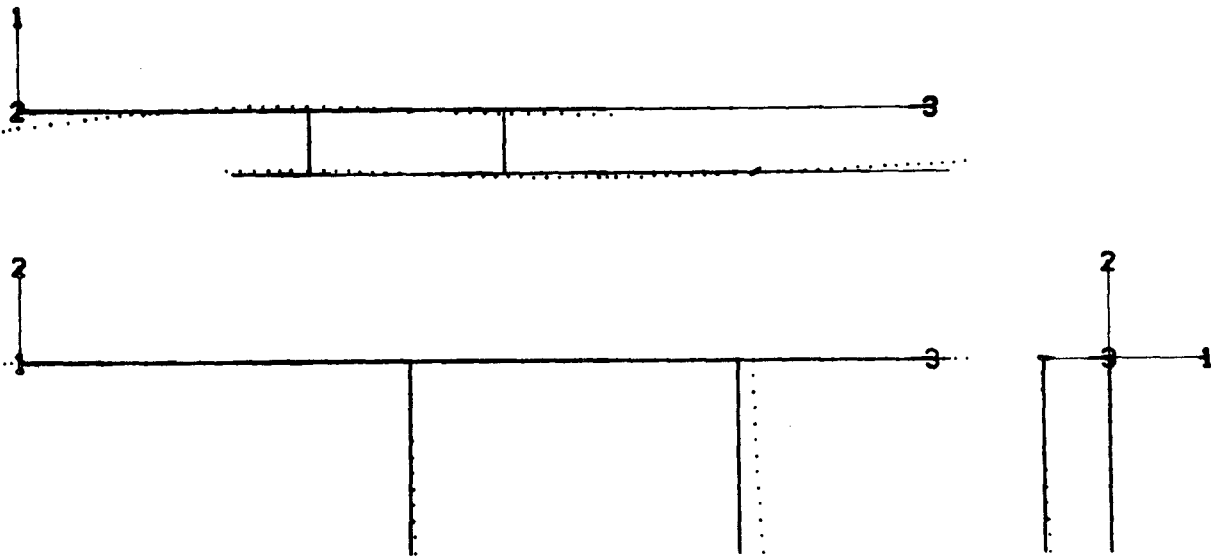


Fig. 7 - Mode 9, Frequency = 7.75 Hz

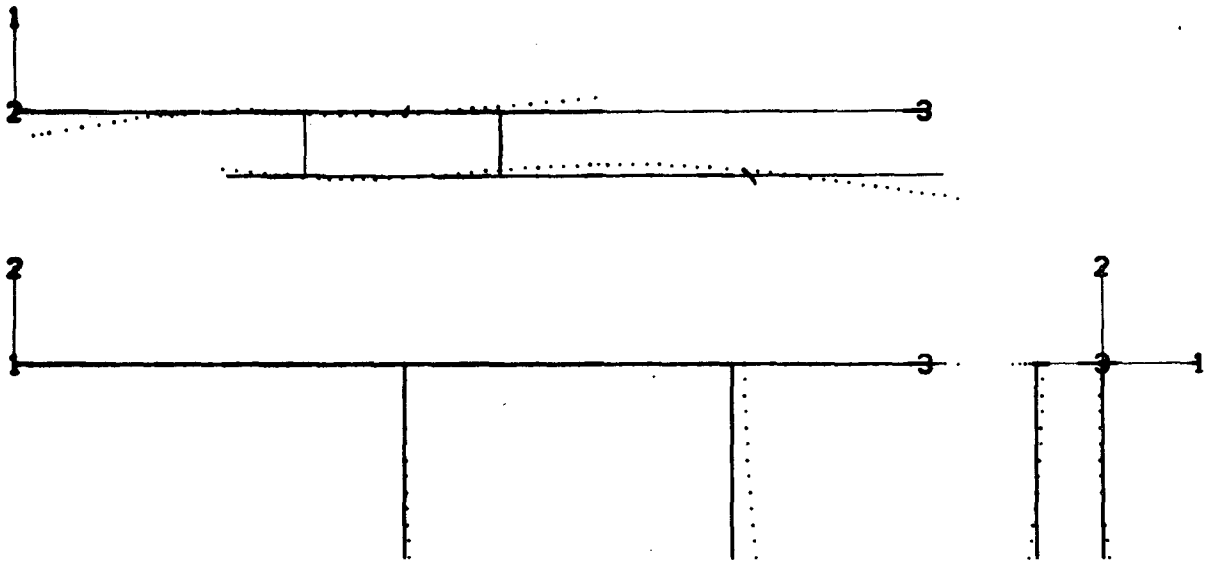


Fig. 8 - Mode 10, Frequency = 9.21 Hz

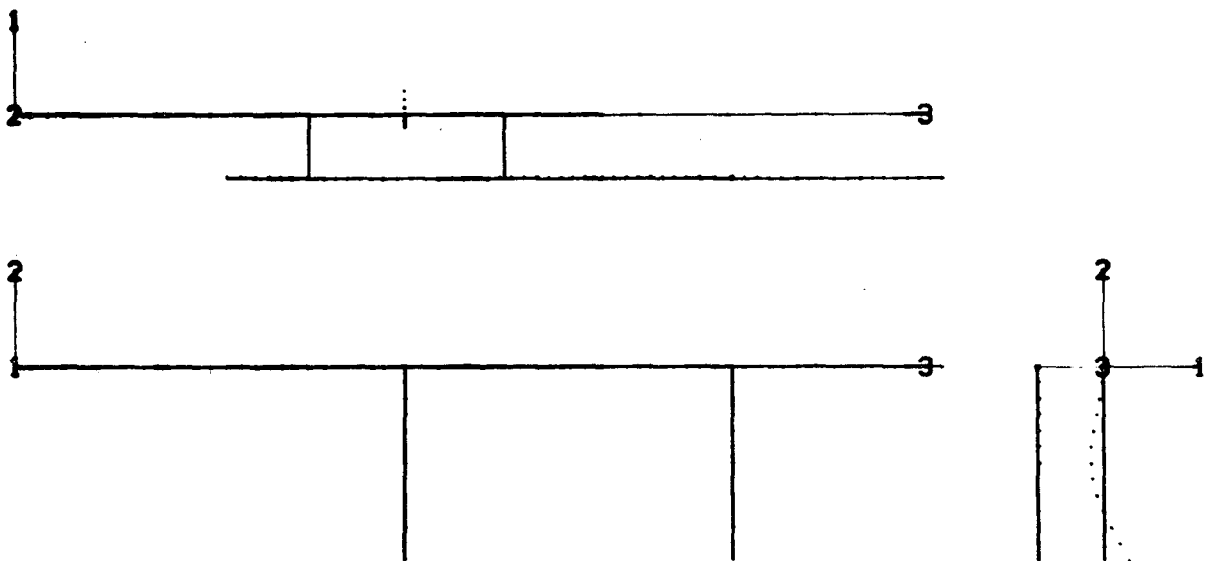


Fig. 9 - Mode 11, Frequency = 11.16 Hz

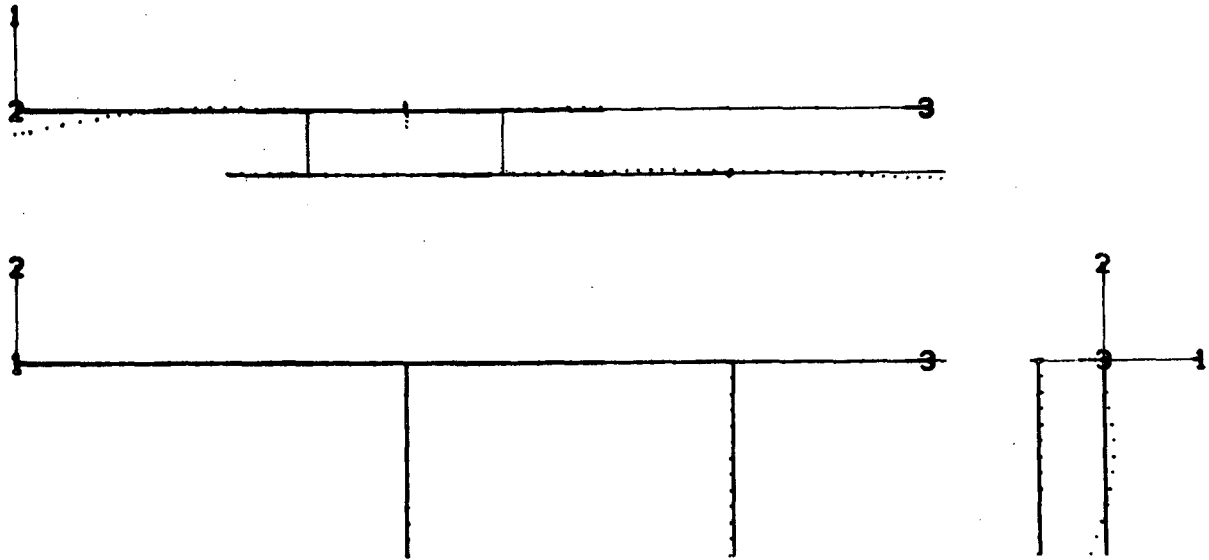


Fig. 10 - Mode 12, Frequency = 11.29 Hz

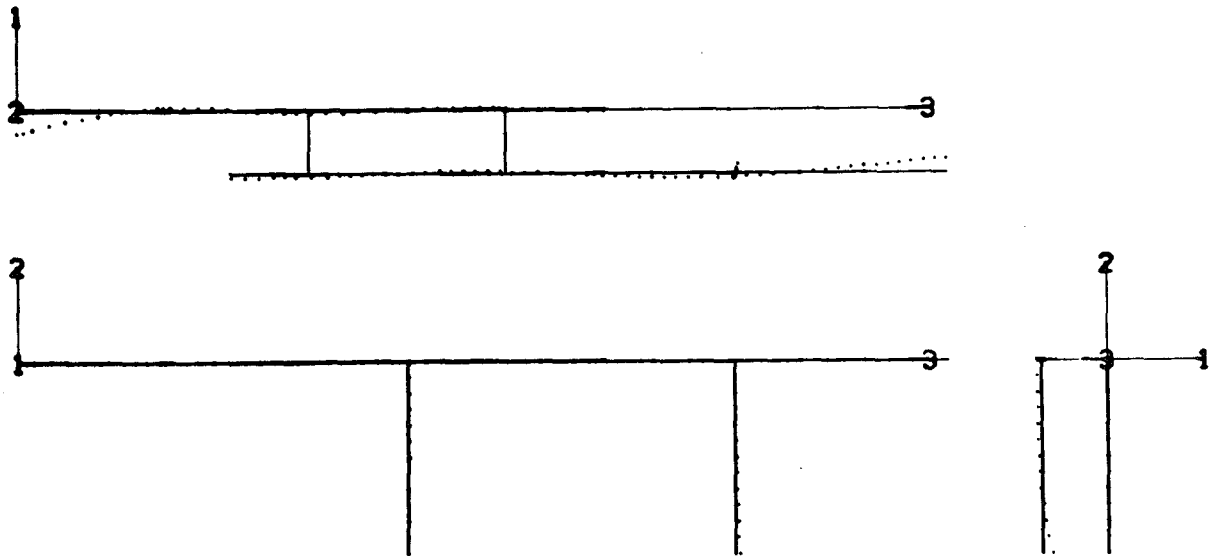


Fig. 11 - Mode 13, Frequency = 14.79 Hz

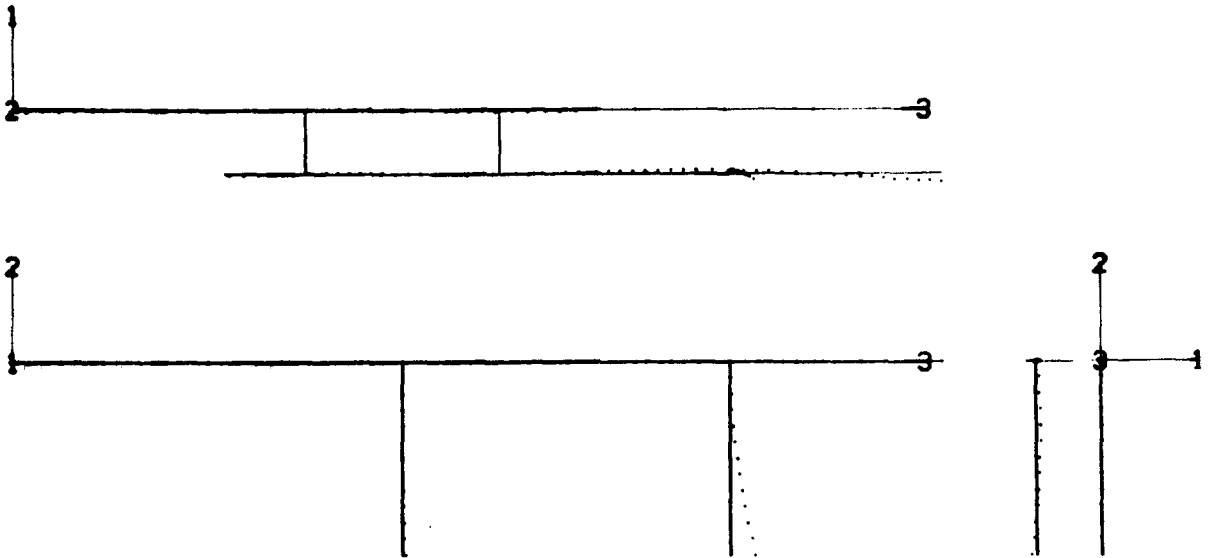


Fig. 12 - Mode 14, Frequency = 16.01 Hz

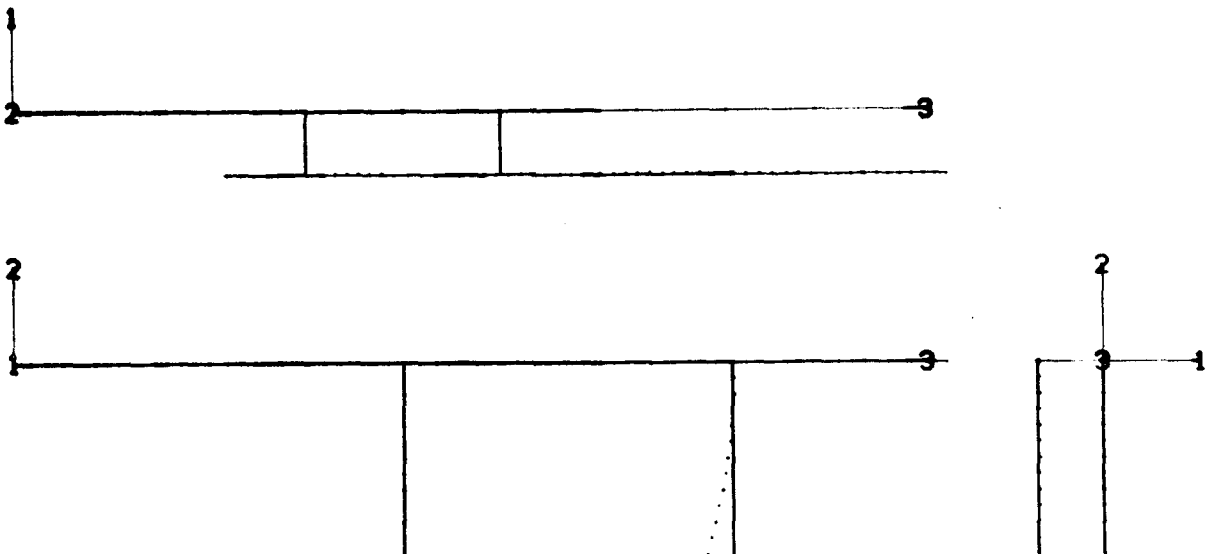
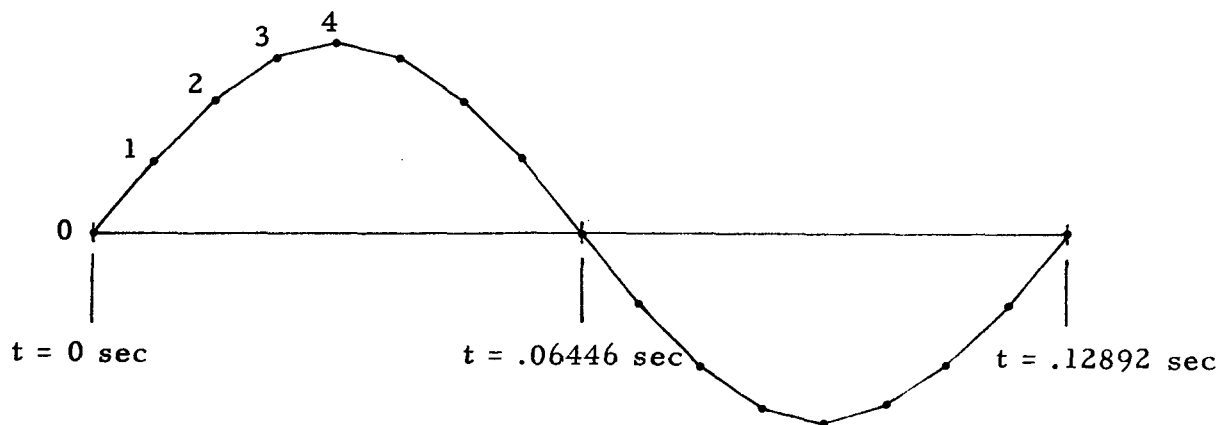


Fig. 13 - Mode 15, Frequency = 17.69 Hz

Section 3

TRANSIENT RESPONSE

The transient response of the space shuttle beam model shown in Fig. 1 was computed with the Substructure Synthesis program for a simulated pogo excitation. A harmonic forcing function in the form of a Z-direction point force was applied at location A (see Fig. 1) of the model. The forcing function is described on Fig. 14. The frequency of the forcing function is equal to the frequency of the ninth system mode as tabulated in Table 2.



	Time (sec)	Magnitude (lb)
0	.00000	0
1	.00806	19134
2	.01611	35355
3	.02417	46194
4	.03223	50000

Fig. 14 - Forcing Function Representation

Mode shapes associated with system modes 4 through 11 (see Fig. 2-9) were used as generalized displacement functions to characterize the response of the system.

For calculating the individual substructure vibrational modes used in determining the system damping matrix, all substructure boundary nodes, except the node located at A (Fig. 1), were completely constrained. Boundary node A was allowed to move freely in the global X-Z plane. Damping factors (see Ref. 1, page B-16) of .005 and .01 were assumed for the first and second modes, respectively, computed for each substructure relative to these boundary node constraints.

The system response, Φ , is expressed as

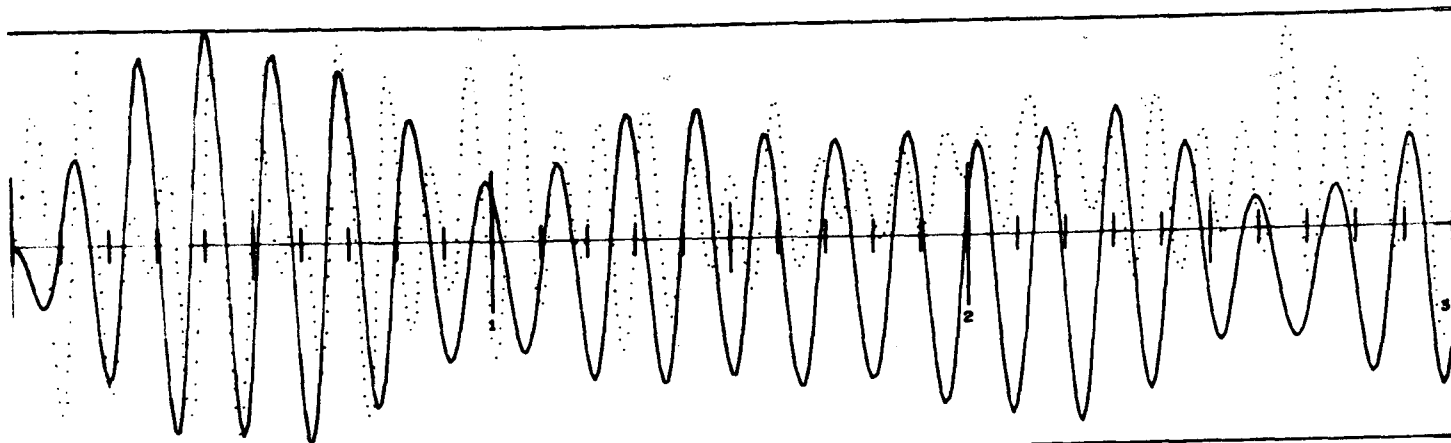
$$\Phi = \sum_{i=1}^n a_i \varphi_i ,$$

where a_i is the coefficient of the i^{th} generalized displacement function, φ_i . Figure 15 illustrates the time histories computed for coefficients of the generalized functions corresponding to system modes 6 through 11 for three seconds of the forced response. Similarly, Fig. 16 illustrates the direction-Z response computed for points A through F shown on Fig. 1. Note that the curves in Fig. 16 are all scaled to the same value (2.03 inches), while the curves in Fig. 15 are scaled individually.

Solid Curve
Coefficient of Mode 8
Max. Value = 0.19

Time in Seconds

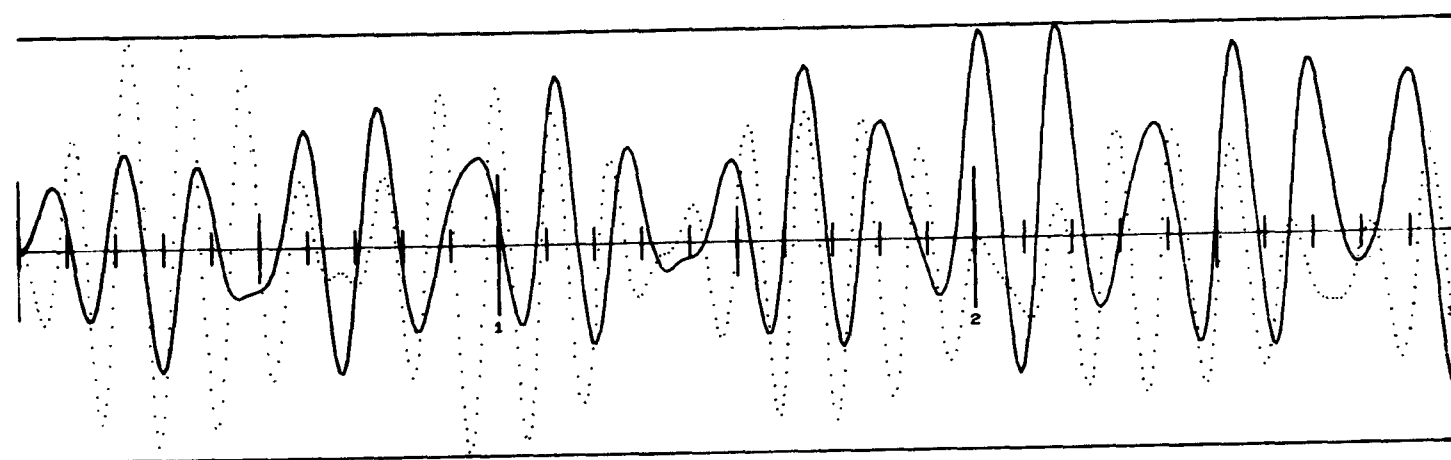
Dotted Curve
Coefficient of Mode 11
Max. Value = 0.30



Solid Curve
Coefficient of Mode 7
Max. Value = 1.09

Time in Seconds

Dotted Curve
Coefficient of Mode 10
Max. Value = 2.33



Solid Curve
Coefficient of Mode 6
Max. Value = 0.17

Time in Seconds

Dotted Curve
Coefficient of Mode 9
Max. Value = 35.34

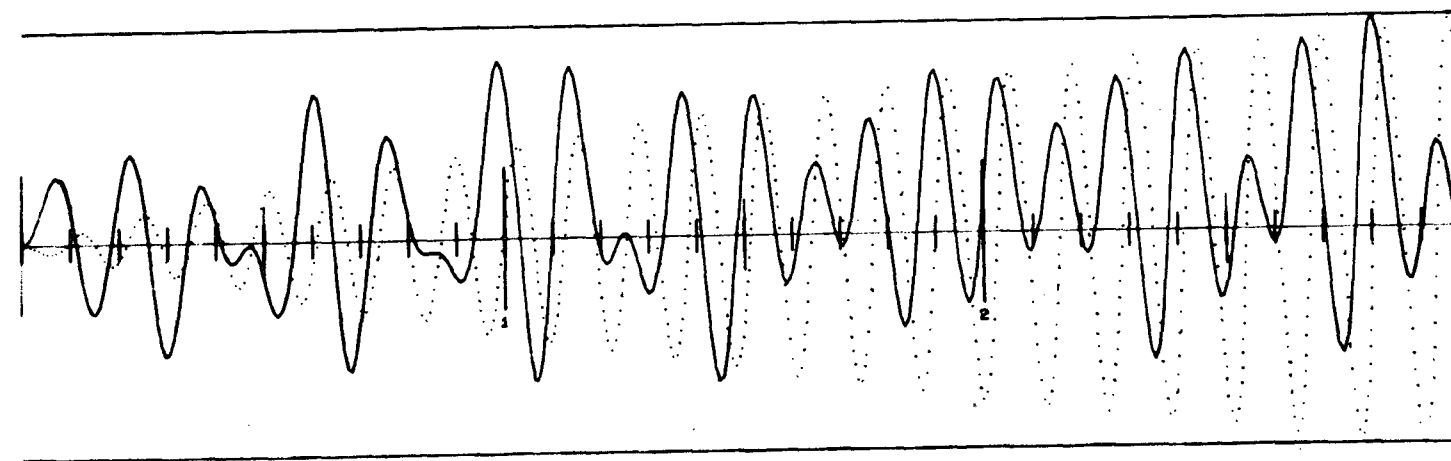


Fig. 15 - Time Histories of Generalized Displacement Function Coefficients

2.03 inches

Solid Curve
Response of Point C

Time in Seconds

Dotted Curve
Response of Point F

-2.03 inches

2.03 inches

Solid Curve
Response of Point B

Time in Seconds

Dotted Curve
Response of Point E

-2.03 inches

2.03 inches

Solid Curve
Response of Point A

Time in Seconds

Dotted Curve
Response of Point D

-2.03 inches

Fig. 16 - Direction-Z Response of Points A-F

LMSC-HREC D162799-A

Section 4

REFERENCES

1. Jones, C. E., "Advanced Substructuring Techniques," Final Report, NAS8-30520, LMSC-HREC D225003, Lockheed Missiles & Space Company, Huntsville, Ala., June 1971.
2. Hurty, W. C., "Dynamic Analysis of Structural Systems by Component Mode Synthesis," JPL TR No. 32-530, Jet Propulsion Laboratory, Pasadena, Calif., January 1964.
3. Hurty, W. C., "Truncation Errors in Natural Frequencies as Computed by the Method of Component Mode Synthesis," Matrix Method in Structural Mechanics, AFFDL-TR-66-80, Wright-Patterson AFB, Ohio, November 1966, pp. 803-822.
4. Whetstone, W. D., "Substructure Uniform Acceleration Modes," Unpublished internal report, Lockheed Missiles & Space Company, Huntsville, Ala., 1967.
5. Jacobs, D. B., "Configuration I SA-501 Dynamic Characteristics," Vol. II, D5-15427-1B, The Boeing Company, Huntsville, Ala., March 1966.
6. Whetstone, W. D., "Free Vibration Characteristics of Saturn I/IB Launch Vehicles," LMSC-HREC A783035, Lockheed Missiles & Space Company, Huntsville, Ala., December 1966.